

# Nano-Ordered Cellulose Containing $I_{\alpha}$ Crystalline Domains Derived from the Algae *Chaetomorpha antennina*

S. Saritha · S.M. Nair · N.C. Kumar

Published online: 1 October 2013  
© Springer Science+Business Media New York 2013

**Abstract** Nano-crystalline cellulose (NCC) with high content of  $I_{\alpha}$  domains are generated by treatment of cellulose microfibrils from the algae *Chaetomorpha antennina* with 80 %  $H_2SO_4$  followed by ethanolic precipitation. X-ray diffraction and FT-IR analyses have revealed that the NCCs produced are highly crystalline and predominantly composed of the  $I_{\alpha}$  allomorph, which indicate the selective dissolution of  $I_{\alpha}$  fragments. AFM images shows that the NCCs produced are of 60–70-nm thickness and of variable length depending on the concentration. The well-dispersed suspension of 1-mg NCC in 10-mL distilled water shows a highly networked structure, which expand its applications over various fields especially in nano-medicine.

**Keywords** Nano-Crystalline Cellulose ·  $I_{\alpha}$  Micro Fibrils · *Chaetomorpha* · Atomic Force Microscopy

## 1 Introduction

Characterization of crystalline allomorphs of cellulose in different class of organisms having significant cellulose content is still an arduous task in carbohydrate chemistry and hence was the subject of several elegant studies. Cellulose microfibrils (CMFs) are minimal-sized crystalline fibres formed by self aggregation of cellulose, the  $\beta$ -1, 4-glucan polymer, in the cell wall of plants, algae and tunica of animals [1–3]. Each of these microfibrils is composed of two crystalline allomorphs with parallel arrangements of the molecular chains that are generally accepted as cellulose  $I_{\alpha}$  and  $I_{\beta}$  [4, 5]. The relative

amounts of  $I_{\alpha}$  and  $I_{\beta}$  have been found to vary between samples from different origins.  $I_{\alpha}$ -rich specimens have been found in the cell wall of some algae and in bacterial cellulose whereas  $I_{\beta}$ -rich specimens have been found in cotton, wood, and ramie fibres [6].

Cellulose  $I_{\alpha}$  and  $I_{\beta}$  have one-chain triclinic and two-chain monoclinic lattices, respectively [7]. The ultra structural localizations of the cellulose  $I_{\alpha}$  and  $I_{\beta}$  allomorphs in a single microfibril had been investigated and two models were proposed. In the first, the two crystalline domains are localized laterally, while in the second, the two domains coexist alternately longitudinally or laterally [4, 8].

Previous results indicated that cellulose  $I_{\alpha}$  was more susceptible to enzymatic degradation than cellulose  $I_{\beta}$  [9]. The cellulose  $I_{\alpha}$ , having more intermolecular hydrogen bonding interaction [10], may enable it to form more cavities in the network. Therefore, the concentration of  $I_{\alpha}$  segments in the sample may be important as it can be used for various applications, especially in medicine as drug delivery vehicle [11].

Therefore, the present study aims to characterise the nano-crystalline cellulose (NCCs) concentrated with  $I_{\alpha}$  crystalline domains obtained from the algal cellulose of *Chaetomorpha antennina* using atomic force microscopy (AFM), x-ray diffraction (XRD) and Fourier transformation-infrared (FT-IR) spectroscopy.

## 2 Experimental

### 2.1 Preparation of Cellulose Substrates

The cell wall cellulose materials were isolated from the green sea-weed *Chaetomorpha antennina* collected from Puthuvypu, Kerala Coast. The substrate was purified by sequential extraction with 0.1-N NaOH at 100 °C for 3 h to remove the organic materials present. The sample separated

S. Saritha · S. Nair (✉) · N. Kumar  
Inter University Centre for Development of Marine Biotechnology  
(IUCDMB), Cochin University of Science and Technology,  
Cochin, India 682016  
e-mail: unnimurali@yahoo.com

by centrifugation was further treated with 0.05-N aqueous HCl at room temperature overnight [15]. Pure cellulose residues were collected as CMFs after homogenization and freeze drying.

## 2.2 Preparation of Nano-crystalline Cellulose

The CMFs obtained were hydrolysed using 40 % (w/w) aqueous H<sub>2</sub>SO<sub>4</sub> solution at room temperature for 3 h with strong stirring and then washed by centrifugation to obtain non flocculating aqueous suspension of micro crystalline cellulose (MCC). This MCC was treated subsequently with 60, 80 % (w/w) H<sub>2</sub>SO<sub>4</sub> at 60 °C by applying strong stirring. A very small concentration remained as larger residues was removed by centrifugation. An excess amount of 99 % ethanol was added to the white-coloured supernatant to yield short nano-crystalline cellulose. The residues which are obtained after centrifugation at 12,000 rpm was thoroughly washed with water and then centrifuged and freeze-dried. The larger residues were repeatedly treated with 80 % H<sub>2</sub>SO<sub>4</sub> until the total weight loss of the sample reached around 75 %. The NCCs obtained were subjected to FT-IR, XRD and AFM analyses to elucidate the composition, crystalline nature and morphology of the sample.

## 2.3 Infrared Spectroscopy

Each sample was mounted on a KBr-thin plate of around 1-mm thickness. FT-IR spectra were obtained from a circular area of 100 μm in diameter using an FT-IR spectrometer. The wave number range scanned was 4,000–650 nm. The internal standard band at 2,900 cm<sup>-1</sup>, assigned to C–H stretching in methyl and methylene groups in the crystalline region was

commonly employed. The relative ratios in cellulose I<sub>α</sub> and I<sub>β</sub> were determined by the intensity ratios of their typical IR bands namely 3,240 for I<sub>α</sub> and 3,270 for I<sub>β</sub> [12].

## 2.4 X-ray Diffraction

X-ray diffraction serves as a non-destructive method for finding the crystal structure and chemical composition of materials and thin films. The degree of crystallinity of the dried NCCs was obtained from the XRD patterns using the x-ray diffractometer (Analytical Xpert Pro.). The orientation of the cellulose fragments also can be assessed based on the angle of diffraction  $2\theta$  [13].

## 2.5 Atomic Force Microscopy

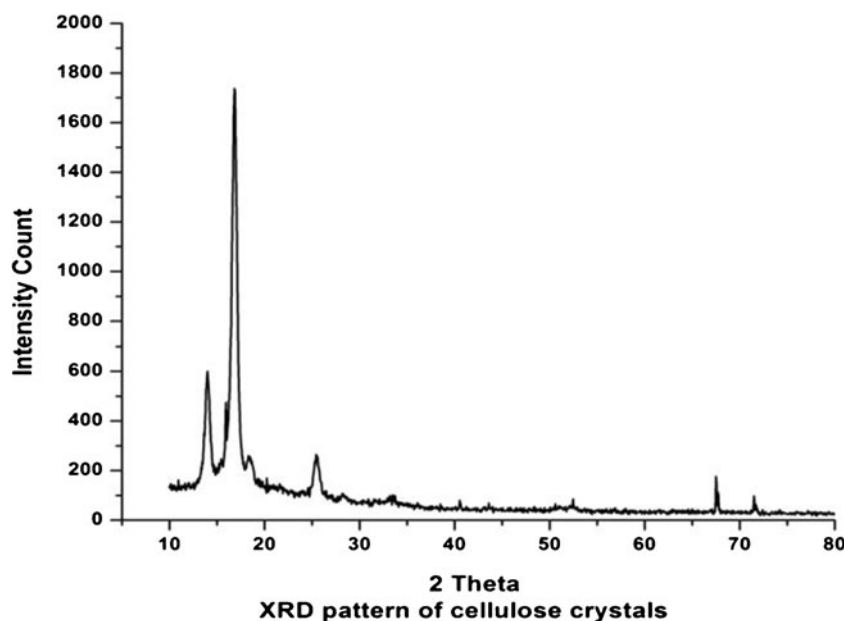
A drop of NCC suspension at different concentrations was deposited on to mica plate (8×8 mm) and then air dried. The samples were observed using a multimode AFM (Agilent 5500) equipped with a scanner having 10-μm range (E scanner). All images (400×400 pixels) were obtained using a tapping mode in air. The cantilever used was 140-μm in length and has an unmodified silicon nitride tip with a spring constant 40 Nm<sup>-1</sup>. The scan rate was 1.5 Hz and the scan angle was varied to obtain optimum contrast.

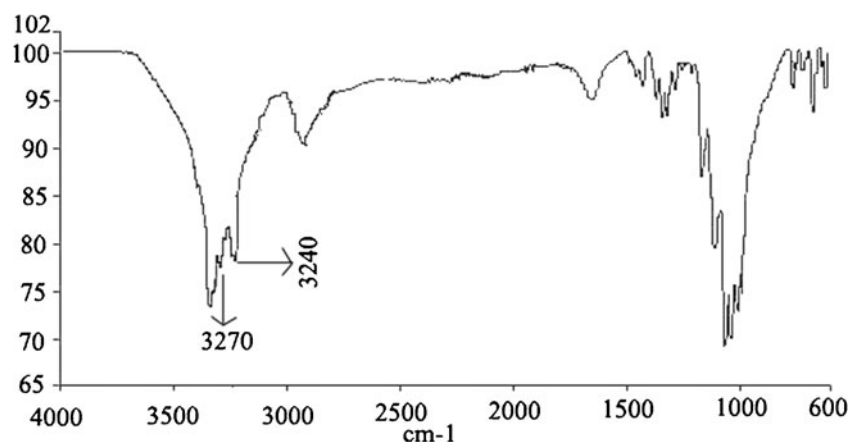
## 3 Result and Discussion

### 3.1 Characterization of the Residues after Acid Hydrolysis

The cellulose micro fibril was acid hydrolysed sequentially to produce nano-crystalline cellulose suspensions and it has been

**Fig. 1** XRD pattern of the NCCs obtained



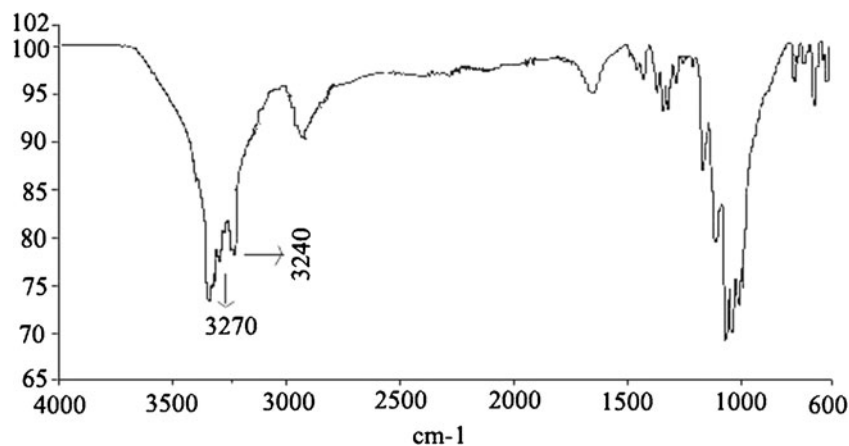
**Fig. 2** IR Spectra of CMF before acid treatment

reported that rheological characterisation of cellulose suspensions showed a viscoelastic solid-like behaviour even at lower concentrations. The yield of these short elements depends on the strength of the acid, stirring time, and the temperature. It is observed that during acid hydrolysis, the yield reached 20–30 % of the initial sample. The larger residues became thinner and/or fibrillated after treatment with 80 %  $\text{H}_2\text{SO}_4$  for 5 h, similar to the case for hydrolysis of  $\text{I}_\beta$ -rich cotton-ramie type cellulose [14]. The lengths of the obtained NCCs changed depending on the concentration.

The x-ray diffractogram of the NCC is shown in Fig. 1. The cellulose suspension obtained after acid hydrolysis exhibited a high degree of crystallinity, indicating that non-crystalline regions may not be present in newly produced NCCs. The very well resolved and narrow peaks are the distinctive properties of the highly crystalline cellulose in XRD, especially at  $2\theta$ s of 14 and 16, which are not common for the native cellulose obtained from higher plants. This indicated a specific uniplanar orientation of the algal cell wall. The degree of crystallinity is as high as 95 %, obtained from XRD. The highly intense peak at 16 indicated the presence of high amount of  $\text{I}_\alpha$  cellulose compared to the  $\text{I}_\beta$  analogue. It has already been investigated that two allomorphs  $\text{I}_\alpha$  and  $\text{I}_\beta$

coexist in the CMFs isolated from the algal cell wall, alternating either longitudinally or laterally. The transition zone between the two phases was found to be the interface between adjacent H-bonded molecular sheets (viz., 0.39-nm lattice planes) [15].

The cellulose  $\text{I}_\alpha$  and  $\text{I}_\beta$  contents in the samples were calculated on the basis of the IR analyses. The initial sample was found to contain around 30 % cellulose  $\text{I}_\beta$  (Fig. 2) as obtained by comparing the peak areas. The NCCs obtained after acid hydrolysis was found to have only 13 % of  $\text{I}_\beta$  which indicated the selective dissolution of  $\text{I}_\alpha$  (Fig. 3). This result also indicated that the acid did not attack the cellulose suspension uniformly during the reaction time course since the  $\text{I}_\alpha$  content differed between the larger residues and NCCs. The FT-IR results suggested that the NCCs were predominantly composed of cellulose  $\text{I}_\alpha$ , although a trace amount of cellulose  $\text{I}_\beta$  was still remained, when the bands in the region of 3,450–3,150  $\text{cm}^{-1}$  [16] were compared before and after the acid hydrolysis. The absorption bands at 3,270  $\text{cm}^{-1}$  due to cellulose  $\text{I}_\beta$  were drastically decreased after the sequential acid hydrolysis. A trace amount of unhydrolyzed cellulose  $\text{I}_\beta$  may still remain at the ends of the NCCs. It is generally accepted that certain treatments are able to convert cellulose  $\text{I}_\alpha$  to cellulose

**Fig. 3** IR Spectra of CMF after acid treatment

$I_{\beta}$ , but they require a high pressure and high temperature [17–19]. In the present study, such conversion could not take place as the conditions applied are not enough for the conversion.

### 3.2 Surface Morphology and the Supramolecular Nature of NCC

The surface morphology of the samples was obtained from AFM which was employed in a tapping mode in air. The NCCs were observed as nano-rods of thickness 60–70 nm. The length of these rods was found to be varying depending on the concentration of the sample. In the lower concentrated samples i.e., 0.1 mg/10 mL, some fragments are found to have a length of 100–200 nm, but some are found to be longer rods of several 1,000-nm length (Fig. 4). This may be due to the supramolecular aggregation of these crystalline cellulose fragments. At concentration of 0.5 mg/10 mL, there was not much difference (Fig. 5), whereas the dispersion of 1 mg of cellulose powder in 10-mL distilled water by ultra-sonication has showed a cluster formation. The nano-crystalline cellulose fragments were produced by the selective dissolution of  $I_{\alpha}$  domains of short range order by treating the CMFs rich in  $I_{\alpha}$  with 80 % sulphuric acid. The selective dissolution may be due to the hydrogen bonding differences between two forms of native cellulose which were already studied computationally [20] and it was clear from O–H...O angles that the hydrogen bonds in  $I_{\beta}$  are distributed over a region of better geometry than those in  $I_{\alpha}$ . The more favourable intrachain H-bonding in  $I_{\beta}$  must be due to the difference in cellulose chain conformation between  $I_{\alpha}$  and  $I_{\beta}$  [21].

Micro crystalline cellulose, which is the purest form of commercially available native cellulose, is one of the most commonly used drug excipients. A recent study suggested that MCC from fodder grass can act as a potential drug carrier for an antituberculosis drug [22]. The large surface area of

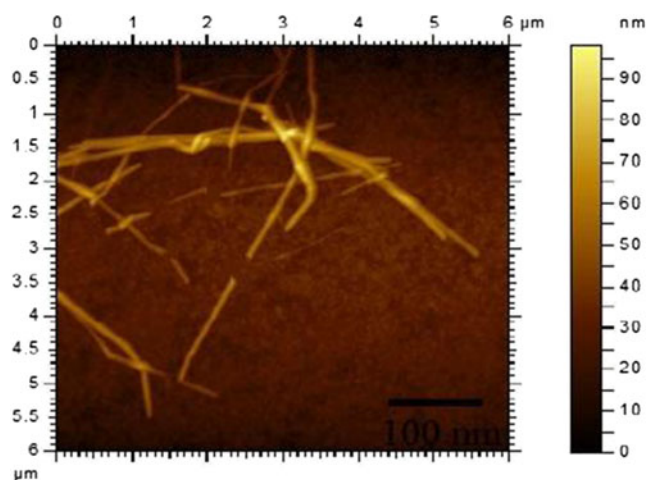


**Fig. 4** AFM images of NCCs of concentration 0.1 mg/10 Ml

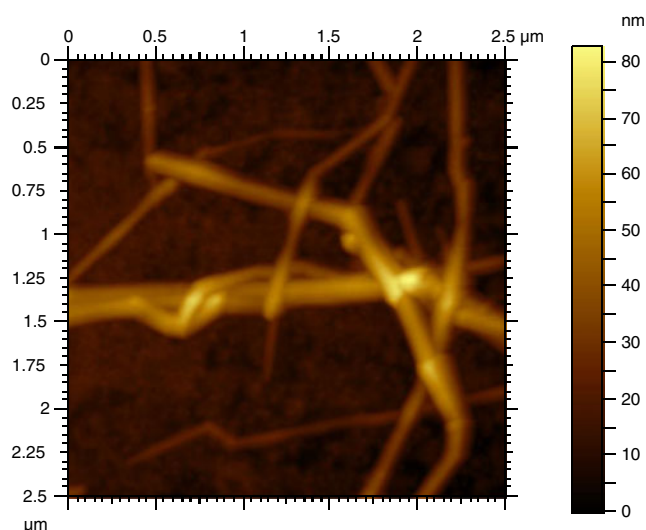


**Fig. 5** AFM images of NCCs of concentration 0.5 mg/10 Ml

*Chaetomorpha* cellulose and its inertness make this material to be used as an alternative to MCC as a drug carrier. In order to observe the changes while improving the concentration, 1 mg of the NCC was well dispersed in 10-mL distilled water by continuous stirring for 30 min and the AFM images were taken by drop casting the solution on mica sheet. The images had shown a nano cluster formation and the fibres are found to maintain almost the same thickness as the lower concentrated solutions viz 60–70 nm (Fig. 6). These clusters, found to have large space inside the network which may be beneficial for it to be used as drug carriers and most probably for several other industrial applications, for example, to improve the performance of polyvinyl acetate as wood adhesive [23].

In conclusion, the controlled acid hydrolysis of *Chaetomorpha* CMFs yielded short elements designated as NCCs with high crystallinity. The NCCs were mainly composed of a cellulose  $I_{\alpha}$  crystalline phase with a width of 70–80 nm and

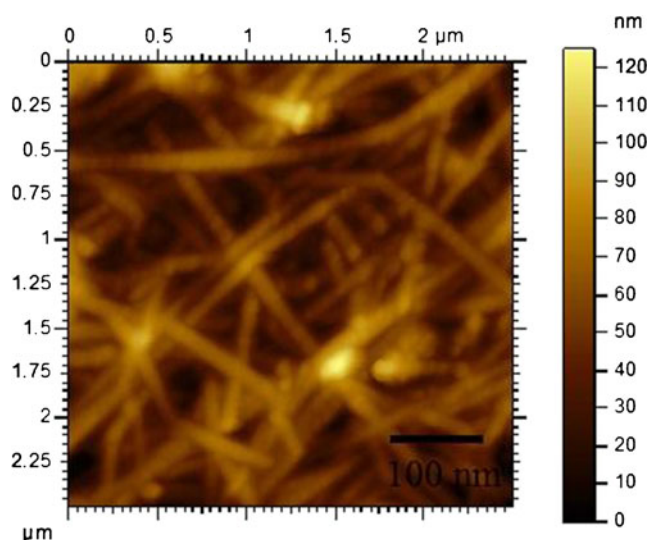


**Fig. 6** AFM images of NCCs of concentration 1 mg/10 mL

the length varied depending on concentration. Acid strength, temperature, and mechanical force applied by stirring the samples during the process also assisted the formation of NCCs. These NCCs have the potential to act as nano-ordered bioparticles and these may be useful in the field of medicine as drug carriers due to the vacant spaces they possess in cluster formation. Also, exploration of the applications of *Chaetomorpha* cellulose is of much importance as green algae so far have found only limited industrial use compared to other classes of algae and these findings may alleviate serious environmental problems associated with seasonal algal blooms.

#### 4 Conclusions

The controlled acid hydrolysis of *Chaetomorpha* CMFs yielded short elements designated as NCCs with high crystallinity. The NCCs were mainly composed of a cellulose  $I_{\alpha}$  crystalline phase with a width of 70–80 nm and the length varied depending on concentration. Acid strength, temperature, and mechanical force applied by stirring the samples during the process also assisted the formation of NCCs. These NCCs have the potential to act as nano-ordered bioparticles and these may be useful in the field of medicine as drug carriers due to the vacant spaces they possess in cluster formation. Also, exploration of the applications of *Chaetomorpha* cellulose is of much importance as green algae so far have found only limited industrial use compared to other classes of algae and these findings may alleviate serious environmental problems associated with seasonal algal blooms.

**Acknowledgments** One of the authors (SS) is grateful to the financial assistance by CSIR (India). We thank Prof. Jayaraj M.K., department of physics, CUSAT for providing the instrumental facilities, and the Government of Kerala for the financial support received to establish a new centre, Inter University Centre for Development of Marine Biotechnology (IUCDMB).

#### References

- Sýturova, I. H., Apperley, D. C., Sugiyama, J., Jarvis, M. C. (2004). Structural details of crystalline cellulose from higher plants. *Biomacromolecules*, *5*, 1333–1339.
- Imai, T., Boisset, C., Samejima, M., Igarashi, K., Sugiyama, J. (1998). Unidirectional processive action of cellobiohydrolase Cel7A on Valonia cellulose microcrystals. *FEBS Letters*, *432*, 113–116.
- Klemm, D., Heublein, B., Fink, H. P., Bohn, A. (2005). Cellulose: fascinating biopolymer and sustainable raw material. *Angewandte Chemie International Edition*, *44*, 3358–3393.
- Sugiyama, J., Persson, J., Chanzy, H. (1991). Combined Infrared and Electron Diffraction Study of the polymorphism of native celluloses. *Macromolecules*, *24*, 2461–2466.
- Horii, F., Hirai, A., Kitamaru, R. (1987). CP/MAS  $^{13}\text{C}$  NMR spectra of the crystalline components of native cellulose. *Macromolecules*, *20*, 2117–2120.
- Hayashi, N., Ishihara, M., Sugiyama, J., Okano, T. (1998). The enzymatic susceptibility of cellulose microfibrils of the algal-bacterial type and cotton-ramie type. *Carbohydrate Research*, *305*, 109–116.
- Yoshiharu, N., Paul, L., Henri, C. (2002). Crystal structure and hydrogen-bonding system in cellulose  $I_{\beta}$  from synchrotron x-ray and neutron fiber diffraction. *Journal of American Chemical Society*, *124*, 9074–9082.
- Sugiyama, J., Okano, T., Yamamoto, H., Horii, F. (1990). Transformation of Valonia cellulose crystals by an alkaline hydrothermal treatment. *Macromolecules*, *23*, 3196–3198.
- Hayashia, N., Kondob, T., Ishiharaa, M. (2005). Enzymatically produced nano-ordered short elements containing cellulose  $I_{\beta}$  crystalline domains. *Carbohydrate Polymers*, *61*, 191–197.
- Nishiyama, Y., Sugiyama, J., Chanzy, H., Langan, P. (2003). Crystal structure and hydrogen bonding system in cellulose  $I_{\alpha}$  from synchrotron x-ray and neutron fiber diffraction. *Journal of American Chemical Society*, *125*, 47.
- Jackson, J. K., Letchford, K., Wasserman, B. Z., Ye, L., Hamad, W. Y., Burt, H. M. (2011). The use of nanocrystalline cellulose for the binding and controlled release of drugs. *International Journal of Nanomedicine*, *6*, 321–330.
- Yamamoto, H., Horii, F., Hirai, A. (1996). In situ crystallization of bacterial cellulose II. Influences of different polymeric additives on the formation of celluloses  $I_{\alpha}$  and  $I_{\beta}$  at the early stage of incubation. *Cellulose*, *3*, 229–242.
- Wada, M., Okano, T., Sugiyama, J. (1997). Synchrotron radiated x-ray and neutron diffraction study of native cellulose. *Cellulose*, *3*, 221–232.
- Elazzouzi-Hafraoui, S., Nishiyama, Y., Putaux, J., Heux, L., Dubrueil, F., Rochas, C. (2008). The shape and size distribution of crystalline nanoparticles prepared by acid hydrolysis of native cellulose. *Biomacromolecules*, *9*, 57–65.
- Mihrianyan, A. (2011). Cellulose from Cladophorales green algae: from environmental problem to high-tech composite materials. *Journal of Applied Polymer Science*, *119*, 2449–2460.
- Barsberg, S. (2010). Prediction of vibrational spectra of polysaccharides simulated IR spectrum of cellulose based on density functional theory (DFT). *Journal of Physical Chemistry*, *11*, 11703–11708.
- Debzi, E. M., Chanzy, H., Sugiyama, J., Tekely, P., Excoffier, G. (1991). The  $I_{\alpha}/I_{\beta}$  transformation of highly crystalline cellulose by annealing in various mediums. *Macromolecules*, *24*, 6816–6822.
- Kose, R., Mitani, I., Kasai, W., Kondo, N. (2011). Nanocellulose as a single nanofiber prepared from pellicle secreted by *Gluconacetobacter xylinus* using aqueous counter collision. *Biomacromolecules*, *12*, 716–720.
- Yamamoto, H., Horii, F., Odani, H. (1989). Structural changes of native cellulose crystals induced by annealing in aqueous alkaline and acidic solutions at high temperatures. *Macromolecules*, *22*, 4130–4132.
- Esrifili, M. D., & Ahmadin, H. (2012). DFT study of  $^{17}\text{O}$ ,  $^1\text{H}$  and  $^{13}\text{C}$  NMR chemical shifts in two forms of native cellulose,  $I_{\alpha}$  and  $I_{\beta}$ . *Carbohydrate Research*, *347*, 99–106.
- Desiraju, G. R., & Steiner, T. (1999). *The weak hydrogen bond*. New York: Oxford University Press.
- Kalita, R. D., Natha, Y., Ochubiojoa, M. E., Buragohain, A. K. (2013). Extraction and characterization of microcrystalline cellulose from fodder grass, *Setaria glauca* (L) P. Beauv, and its potential as a drug delivery vehicle for isoniazid, a first line antituberculosis drug. *Colloids and Surfaces B*, *108*, 85–89.
- Kaboorani, A., Riedl, B., Blanchet, P., Fellin, M., Hosseinaei, O., Wang, S. (2012). Nanocrystalline cellulose (NCC): a renewable nano-material for polyvinyl acetate (PVA) adhesive. *European Polymer Journal*, *48*, 1829–1837.